Vol. 599: 19–34, 2018
https://doi.org/10.3354/meps12645

MARINE ECOLOGY PROGRESS SERIES
Mar Ecol Prog Ser

Published July 12

Phases of microalgal succession in sea ice and the water column in the Baltic Sea from autumn to spring

Sara Enberg[1,2,*], Markus Majaneva[1,2,3], Riitta Autio[4], Jaanika Blomster[2], Janne-Markus Rintala[1,2,5]

[1]Tvärminne Zoological Station, University of Helsinki, J.A. Palménin tie 260, 10900 Hanko, Finland
[2]Department of Environmental Sciences, University of Helsinki, PO Box 65, 00014 Helsinki, Finland
[3]Department of Natural History, NTNU University Museum, Norwegian University of Science and Technology, 7491 Trondheim, Norway
[4]Marine Research Centre, Finnish Environment Institute, PO Box 140, 00251 Helsinki, Finland
[5]INAR – Institute for Atmospheric and Earth System Research, University of Helsinki, PO Box 64, 00014 Helsinki, Finland

ABSTRACT: The phytoplankton biomass in the Baltic Sea is low during the cold-water season (October to May) compared to the warm-water season (June to September). However, the sea ice is a habitat for diverse assemblages in polar and subpolar areas. These areas, including the Baltic Sea, are subject to changing environmental conditions due to global warming, and temporal and spatial studies are required to understand changes in the processes the organisms are involved in. We delineated microalgal succession in the northern Baltic Sea during the cold-water season using a weekly collected data set. Microscopy results together with molecular methods showed that 5 microbial groups could be distinguished: the sea-ice microalgal assemblage and 4 phytoplankton assemblages (fall, winter, under-ice water and spring). Based on cell enumeration, the microalgal biomass in the water column remained low until the end of the ice-covered season and was dominated by small flagellates and dinoflagellates. The young-ice assemblage in January resembled the water-column assemblage, but indicated a partly selective species-concentrating mechanism during ice formation due to lower species richness in ice than in the water column. Biomass of microalgae increased in the ice and water column during the March to May period, and the assemblage changed from flagellate-dominated to diatom- and dinoflagellate-dominated. The result that the spring phytoplankton, based on species and biomass, formed a separate assemblage indicates that sea-ice algae did not contribute to the spring bloom phytoplankton assemblage.

KEY WORDS: Microalgae · Cold-water season · Succession · Sea ice · Baltic Sea

INTRODUCTION

Phytoplankton succession studies in the Baltic Sea have focused on the high-growth season (from spring to fall) (e.g. Niemi 1973, Andersson et al. 1996, Klais et al. 2013, Lips et al. 2014, Svedén et al. 2016). The classical temperate phytoplankton succession description begins in spring, when increasing light enhances primary production and the spring bloom diatoms exhaust nutrients from the water column (Lips et al. 2014). Changes in phytoplankton assemblages follow the changes in the physical environment, i.e. available light and nutrient supply (Popova et al. 2010), but also species interactions, such as competition and grazing (Sommer et al. 1986). A low-production phase with small flagellated algae follows

*Corresponding author: sara.enberg@gmail.com

in the summer, but summertime diazotrophic cyanobacterial blooms are a recurrent phenomenon in eutrophic waters (Finni et al. 2001, Kahru et al. 2007, Svedén et al. 2016). During the fall, when the temperature decreases and stratification is broken, nutrients are replenished and a bloom of diatoms and dinoflagellates may occur (Wassmund & Uhlig 2003). The wintertime in high-latitude seas is characterized by low algal biomass and a predominance of small mixotrophic and heterotrophic taxa (Dale et al. 1999, Moreau et al. 2010, Nicolaus et al. 2012, Krawczyk et al. 2015, Makarevich et al. 2015).

Parallel to the seasonal succession of phytoplankton in high-latitude seas, an annual primary succession occurs in the sea ice, with organisms living in the water column colonizing newly formed sea ice (Lizotte 2003). The initial algal colonization of sea ice has been described as both a non-selective and selective concentrating mechanism during ice formation (Garrison et al. 1983, Gradinger & Ikävalko 1998, Tuschling et al. 2000, Różańska et al. 2008). In laboratory experiments, the transition from open-water to sea-ice habitat is characterized by an initial physiological inhibition, followed by subsequent adaptation (Grossmann & Gleitz 1993).

Based on time series data, a recent review (Leu et al. 2015) suggested a division of sea-ice assemblages into 3 functional phases (pre-bloom, bloom and post-bloom), mostly driven by allogenic factors such as temperature and light. Flagellates, likely heterotrophic (Mikkelsen et al. 2008, Różańska et al. 2009), predominate in the pre-bloom. Towards spring, the increasing solar angle and air temperature diminish the snow cover, increase the ice temperature and enlarge the brine channels (Golden et al. 1998), providing more light and space for ice algae to grow. Photosynthetic diatoms and dinoflagellates dominate in the sea-ice bloom (Stoecker et al. 1992, Gleitz et al. 1998, Ratkova & Wassmann 2005, Mikkelsen et al. 2008). The arborescent colony-forming pennate diatom *Nitzschia frigida* is a key species of land-fast ice across circum-Arctic regions (Syvertsen 1991, Różańska et al. 2009, Poulin et al. 2011). A heterotrophic assemblage characterizes the post-bloom (Haecky & Andersson 1999, Kaartokallio et al. 2008, Riedel et al. 2008). Most of the previous sea-ice related research has focused on the bloom and post-bloom assemblages (Stoecker et al. 1993, Sime-Ngando et al. 1997, Kaartokallio 2004, Thomson et al. 2006, Różańska et al. 2009), and little is known of the flagellate-dominated pre-bloom (Niemi et al. 2011).

Furthermore, comprehensive long-term studies are needed to understand the algal processes that occur in various polar marine ecosystems, which are more likely to be subjected to changing environmental conditions due to global warming, especially during the winter season. However, findings that environmental conditions (mainly ice extent; Legrand et al. 2015, Beall et al. 2016) and assemblage composition (Kremp et al. 2008, Majaneva et al. 2012a) during the winter season govern the magnitude and composition of the phytoplankton spring bloom demand more research. The pelagic and ice-algal assemblages of the Arctic and Antarctic differ from those in the low-salinity Baltic Sea, but the biota originates from the same evolutionary lineages and experiences the same physical conditions (low light and temperature, salinity) during the winter season, and it is therefore likely that similar phenologies occur.

Our paper describes phytoplankton and sea-ice assemblage succession and species dynamics in the water column, under-ice water (UIW) and sea ice during a cold-water and ice-covered season in the northern Baltic Sea. The succession of 2 different sites is described, with different sea-ice cover probabilities, starting from late autumn with open water until the end of the phytoplankton spring bloom. Based on changes in microalgal assemblage composition (microscopy cell enumeration and molecular methods) we divided the microalgae of the cold-water season into different groups based on algal assemblage composition, discuss the interactions among the groups and link the ice-algal assemblage with the phytoplankton spring bloom assemblage.

MATERIALS AND METHODS

Study site and field sampling

Our study was carried out in the northwest of the Gulf of Finland, Baltic Sea. Two different locations were selected as study sites. Krogarviken (Site A; 59° 50.650′ N, 23° 15.100′ E) is a semi-enclosed shallow bay with average water depth of only 3 m. The site has high sea-ice probability and an sea-ice breakup events are unlikely during the ice-covered season. Storfjärden (Site B; 59° 51.250′ N, 23° 15.815′ E), is approximately 30 m deep and more exposed to heavy winds, which can easily cause sudden sea-ice breakups. Sampling was carried out from 8 Oct 2012 to 20 May 2013, with the exceptions of 24 and 31 Dec 2012 and of 22 Apr 2013 when the sea ice started to melt. In addition, due to poor sea-ice conditions, samples could not be collected from Site B on 7 Jan 2013 or 11 and 18 Feb 2013.

Three replicate water samples were taken from each site (A: 0–3 m; B: 0–15 m) using 3 and 15 m long hose samplers (6 cm internal diameter). The cutoff of 15 m at Site B was chosen as a typical depth scale for the euphotic zone (Luhtala & Tolvanen 2013). Water samples were collected into 2 l transparent plastic bottles without any pre-filtration. After sea ice had formed, 3 snow thicknesses on the ice were measured from 3 random spots with 1 cm precision, followed by ice sampling using a motorized CRREL-type ice-coring auger (9 cm internal diameter; Kovacs Enterprises). Sea-ice temperatures were measured at 5 cm intervals using a Testo 110 thermometer, and sea-ice thicknesses were measured from the obtained ice cores before they were placed in plastic tubing (Mercamer Oy). Three replicate ice samples were taken from each site. For one replicate ice sample, 2 to 5 entire ice cores, depending on the ice thickness, were drilled and pooled to ensure there was enough melted sea ice to be comparable to the 2 l water samples. In addition, 3 replicate UIW samples were collected from the drill hole by submerging the 2 l plastic sample bottle under the water's surface. Water temperature and salinity were measured using a Falmouth Scientific NXIC CTD. All water and sea-ice samples were kept in the dark during transportation to the field station, where the sea-ice samples were crushed and melted without allowing the temperature of the sample to rise above +4°C, as explained in Rintala et al. (2014). The melting method used in this study also avoids salinity shock in ice algal assemblages, which was statistically shown at the same site by Rintala et al. (2014). After this, the ice samples were treated in the same way as the water samples. The bulk salinities of the melted sea-ice samples were measured with an YSI 63 meter (Yellow Springs Instruments).

Nutrients

For nutrient analysis, 1000 ml of water from each 3 replicates was pooled into one sample. Both inorganic (NH_4, NO_2+NO_3, PO_4 and SiO_4) and total nutrient (tot-N and tot-P) concentrations were determined using a Hitachi U-110 Spectrophotometer (Hitachi High-Technologies) with standard protocols for seawater analysis (Koroleff 1976). Ice nutrient concentrations were normalized to the mean bulk salinities of melted sea ice to correct for salinity-related variations in the nutrient concentrations.

Chlorophyll *a* measurements

For measuring chlorophyll *a* (chl *a*) concentration, two 100 ml subsamples were taken from every water and ice sample. They were filtered onto GF/F filters (Whatman), soaked in 96% v/v ethanol and kept in darkness overnight to extract chl *a* (HELCOM 1988). The chl *a* concentration was calculated from the chl *a* fluorescence measured with a Cary Eclipse spectrofluorometer (Varian/Agilent Technologies) calibrated with pure chl *a* (HELCOM 1988). The chl *a* concentrations for ice were converted to mg m^{-3} of sea ice by multiplying the chl *a* concentration of the meltwater by a standard sea ice to seawater density ratio (917 kg m^{-3} / 1020 kg m^{-3} = 0.9) as explained in Meiners et al. (2012).

Microalgal identification, cell enumeration and biomass estimation

For microalgal identification, 200 ml subsamples were collected into brown glass bottles from every sample, preserved with acid Lugol's solution and stored refrigerated in darkness until microscopic enumeration. Only one of the 3 replicates was used for the microalgal identification, cell enumeration and biomass estimation. Depending on the sample's microalgal density, a volume of 50 or 10 ml was allowed to settle for 24 h, according to Ütermöhl (1958), and examined with a Leica DM IL, Olympus CK30 or Olympus CKX41 inverted light microscope equipped with 10× oculars and 10 or 40× objectives (Leica Microsystems; Olympus Corporation). More than 50 µm large cells and colonies were counted with 100× magnification over an area covering one-half of the cuvette, and the abundance of single-celled and small taxa was counted from 50 random fields with 400× magnification. Species with morphological characteristics visible in an inverted microscope (e.g. with easily recognizable colony structure and cell shape) were identified to species level, whereas microscopically unidentifiable species were left to a general level. Species easily misidentified (*Gymnodinium corollarium*, *Biecheleria baltica* and *Apocalathium malmogiense*) due to similar gross morphology were identified as the '*Scrippsiella*' complex in the acid Lugol's fixed samples. The cell numbers were converted into carbon biomasses (mg C m^{-3}) using species-specific biovolumes and carbon contents according to Olenina et al. (2006) and Menden-Deuer & Lessard (2000). The biomass was converted to mg m^{-3} of sea ice in a similar manner as the chl *a* concentration used for ice (see above).

DNA isolation and 18S rRNA gene identification

For the DNA extraction, 500 or 1000 ml of water and melted sea ice was sequentially filtered using 47 mm diameter 180 µm pore-size nylon filters (Merck Millipore), 20 µm Polyvinylidene fluoride filters (Durapore©, Millipore) and 0.2 µm mixed cellulose ester membrane filters (Schleicher and Schuell Bioscience). The filters were stored in a −80°C freezer until further processing. Total DNA was extracted from the 0.2 µm filters using a PowerSoil® DNA Isolation Kit (MO BIO Laboratories).

PCR amplification was carried out in 2 stages following Koskinen et al. (2011). In brief, the V4 region of the 18S rRNA gene was amplified using Phusion polymerase (Finnzymes) and forward primer E572F (Comeau et al. 2011) with truncated Illumina 5′ overhang 5′-ATC TAC ACT CTT TCC CTA CAC GAC GCT CTT CCG ATC T-3′ and reverse primer 897R (Hugerth et al. 2014) with 5′ overhang 5′-GTG ACT GGA GTT CAG ACG TGT GCT CTT CCG ATC T-3′. Cycling conditions consisted of an initial denaturation at 98°C for 30 s, 20 cycles of 98°C for 10 s, 65°C for 30 s and 72°C for 10 s, and a final extension for 5 min. The amplification was completed in 3 replicates during the second stage, using a full-length Illumina P5 adapter and Indexed P7 adapters. The replicates were pooled between and after the amplifications. The PCR products were purified using AMPure XP beads (Beckman Coulter) and quantified with Qubit (Invitrogen). The amplicons were paired-end sequenced on an Illumina MiSeq instrument using a v3 600-cycle kit (Illumina) at the Institute of Biotechnology (Helsinki, Finland).

The resulting reads were processed using usearch v.8.1.1831_win32 (Edgar 2013). For details of the methods, see Supplement 1 at www.int-res.com/articles/suppl/m599p019_supp.txt. In brief, the paired-end reads were merged using -fastq_mergepairs and quality-filtered using a -fastq_filter with a minimum read length of 200 bases and a 1.0 maximum expected error rate. The primer sequences were removed and the reads were dereplicated, using -derep_fulllength. Singletons were removed and operational taxonomic units (OTUs) were clustered at a 97% similarity level, using -cluster_otus. The above steps were performed for each sample, and the resulting OTU fasta-files were pooled using merge.files in mothur v.1.36.1 (Kozich et al. 2013). The OTUs were then sorted based on the abundance of reads assigned to them, using usearch command -sortbysize. To remove duplicate OTUs stemming from taxa present in several samples, the merged OTUs were re-clustered at a 97% similarity level, using -cluster_otus -minsize 2. The abundance of each OTU in each sample was resolved, using -usearch_global against the pooled OTU file. This pipeline was developed based on an analysis of a mock assemblage and 7 negative PCR reactions sequenced together with the samples (M. Majaneva unpubl. data). The identity of the 97% OTUs was searched, using classify.seqs in mothur against the PR^2 reference library (Chevenet et al. 2006, 2010, Guillou et al. 2013) and using blastn search in BLAST v.2.3.0+ (Zhang et al. 2000) against a nucleotide database at the National Center for Biotechnology Information (NCBI), followed by the lowest common ancestor algorithm in MEGAN6 (minimum bit score 400, top percentage 3.0 and minimum support 1; Huson et al. 2016). Taxonomy was assigned based on an agreement between the 2 searches. In the absence of a taxonomic assignment, the OTU was treated as unclassified and removed from further analyses as a putative chimera (372 OTUs).The OTUs assigned as metazoa, land plants and land fungi were also removed for the downstream analyses (41, 10 and 38 OTUs, respectively), and the number of reads/sample was normalized to 27 591. Diversity metrics (abundance-based coverage estimator [ACE], Shannon and inverse Simpson's indices based on OTU abundance) were calculated, using the summary.single command in mothur. The raw reads were submitted to the Sequence Read Archive of the European Nucleotide Archive's (ENA) with accession number PRJEB21047.

Statistical methods

One-way analysis of variance (ANOVA) was used to test the significance of the differences between the sites and between ice and water for chl *a* and diversity metrics. Levene's test was used to test the homogeneity of variances and Shapiro-Wilk test to test the assumption of normality of the data. A parametric ANOVA and Tukey's *b* test in pairwise comparisons were used when the variances were homogenous, while a non-parametric Kruskal-Wallis test with ranked data and the Mann-Whitney *U*-test were used when the variances were unequal. The correlation between algal biomass and chl *a* concentrations was analysed with Spearman's rank-order correlation. For all tests, $p < 0.05$ was considered statistically significant. The procedures were performed in SPSS for Windows v.23 (IBM).

To divide assemblages from the OTU and microscopy analyses into different groups, the PRIMER v.6.1 package of the Plymouth Marine Laboratory

and the programme PAST v.3.04 (Hammer et al. 2001) were used to perform the multivariate analyses (71 samples). Microalgae and OTUs observed more than once in at least 2 samples were included in the analyses to ensure sufficient data for ordination, thus reducing the total number of taxa from 76 to 40 (microalgae) and from 1137 to 661 (OTUs). Data on algal biomasses and OTU abundance were log(x + 1) transformed to produce a less severe difference between small and large values. Groups were defined *a priori* based on substrate and time (water-ice, fall-winter-spring) and hierarchical cluster analysis was conducted on the taxon composition between the samples (Bray-Curtis' similarity index) and tested for significant differences using 1-way PERMANOVA with 9999 permutations (Anderson 2001).

RESULTS

Environmental dynamics

Winter 2012–2013 was characterized by long-lasting ice cover, from mid-December to mid-April on the coast of the Gulf of Finland (http://en.ilmatieteenlaitos.fi/ice-winter-2012-2013). The thermal winter (when the daily mean temperature remains below 0°C) began on 29 Nov 2012 in the sampling area and ended 11 Apr 2013. A short warm period occurred between 27 Dec 2012 and 4 Jan 2013, during which the mean temperature was above 0°C. The heaviest rains were observed between October and December, and snow cover was permanent from 29 Nov 2012 until 18 Apr 2013 (see Fig. S1 in Supplement 2 at www.int-res.com/articles/suppl/m599p019_supp.pdf).

At the beginning of our study, the water column was mixed and the temperature was approximately +11°C at both sites. The temperature decreased towards ice formation, and was close to 0°C throughout the water column during the ice-covered season. After ice melt, the water temperature increased, and on 20 May 2013 thermal stratification was established at both sites (see Fig. S2 in Supplement 2). Before ice formation, the salinity was approximately 5.5 at Site A and 6.0 at Site B. Salinity decreased during the ice-covered season, and was 3.5 to 5 at Site A and 4.7 to 5.7 at Site B. After ice breakup, the salinity was higher compared to the ice-covered season (4.6 to 5.6 at Site A and 5.5 to 5.9 at Site B) (Fig. S3 in Supplement 2).

The ice conditions differed between the 2 sites. The ice cover at Site A formed at the end of 2012 and broke up after mid-April 2013. The first ice samples were collected on 7 Jan 2013, when ice thickness was 9 cm. A maximum ice thickness of 47 cm was reached at the beginning of April (Fig. 1a). The first ice samples from Site B were collected on 14 Jan 2013, when ice thickness was 11 cm. The weather conditions changed in mid-February, and strong winds broke up the ice. Samples were collected again on 28 Feb 2013, when the ice field was reformed from old ice floes either singly or by being packed on top of each other. There was also new ice that had formed between the old ice floes, but this ice was not sampled. The ice reached a maximum thickness of 53 cm at the end of March, and Site B was ice-free in mid-April 1 wk prior to Site A (Fig. 1b). Snow cover thickness varied from 0 to 19 and 0 to 3 cm at Sites A and B, respectively (Fig. 1).

The concentrations of NH_4-N, NO_2+NO_3-N, PO_4-P, SiO_4-Si and tot-N and tot-P concentrations in the ice were lower compared to those in the water column, except for NH_4-N, which was higher in the ice and UIW compared to the 0–3 m and 0–15 m layers at Sites A and B, respectively. After ice breakup, the PO_4-P and SiO_4-Si concentrations decreased in the water column and the NO_2+NO_3-N concentration was zero. The tot-N and tot-P concentrations showed a small decrease after ice breakup (see Table S1 in Supplement 2).

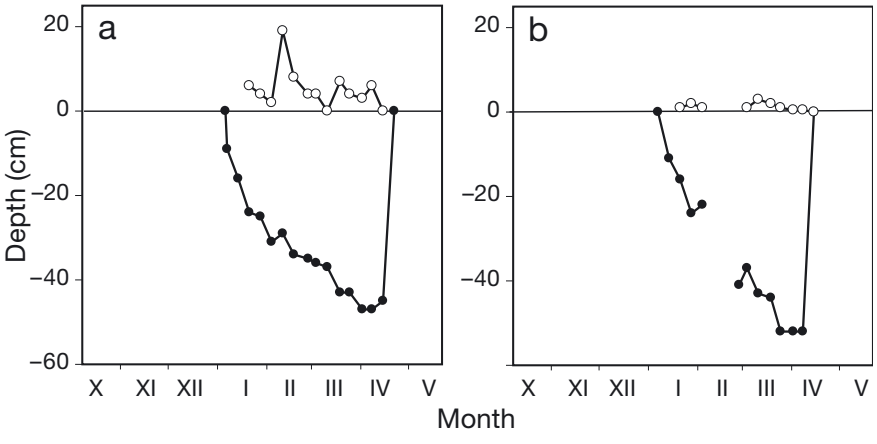

Fig. 1. Mean snow (white circles) and ice (black circles) depths at (a) Krogarviken (Site A) and (b) Storfjärden (Site B). Depth of 0 cm: ice surface

Seasonal dynamics of chl *a* and the microalgal assemblages

The chl *a* concentration in the water column was low from the beginning of the study until April, and the maximum concentration was 6 mg chl *a* m^{-3} at both sites (Fig. 2). The ice chl *a* concentration differed significantly between the 2 sites throughout the ice-covered season (Kruskal-Wallis test, Mann-Whitney *U*-test, all $p < 0.05$). The chl *a* concentration in the ice at Site A increased from 4.4 ± 0.3 mg chl *a* m^{-3} at the beginning of the ice-covered season to 32.0 ± 3.8 mg chl *a* m^{-3} by 8 Apr 2013, after which the chl *a* concentration decreased in the ice and subsequently increased in the UIW and 0–3 m layer. The highest ice chl *a* concentration at Site B (18.9 ± 1.8 mg chl *a* m^{-3}) was observed on 28 Feb 2013, after reformation of the ice field. After 28 Feb 2013, the ice chl *a* concentration decreased towards ice breakup, and was 6.5 ± 0.4 mg chl *a* m^{-3} on 8 Apr 2013. Although the chl *a* concentration at Site B increased in the UIW and 0–15 m layer during the spring, the maximum concentration was similar to that in the ice. During the phytoplankton spring bloom, between 13 and 20 May 2013, the chl *a* concentration was significantly higher in the water column at Site A than at Site B (Kruskal-Wallis test, Mann Whitney *U*-test, all $p < 0.05$) (Fig. 2).

Similar to the chl *a* concentration, total biomass of microalgae based on cell enumeration was low in the water column throughout the cold-water season. The total microalgal biomass at the beginning of the study was 80 mg C m^{-3} at both sites, and decreased to less than 10 mg C m^{-3} during December (Fig. 3). The total biomass in the ice was higher compared to the water column from the beginning of February at Site A and after 28 Feb 2013 at Site B until 8 Apr 2013 (Fig. 3). The total biomass of microalgae in the ice differed between the 2 sites throughout the ice-covered season (January to mid-April). Total biomass in the ice at Site A was 42 to 98 mg C m^{-3} in January and increased to 240 mg C m^{-3} on 28 Feb 2013. The total biomass of microalgae in the ice decreased during March, but increased again in April; highest total biomass (280 mg C m^{-3}) was observed 2 Apr 2013 at Site A. Total biomass of microalgae in the ice at Site B was below 40 mg C m^{-3} in January and February before the ice breakup. Highest total biomass in ice (290 mg C m^{-3})

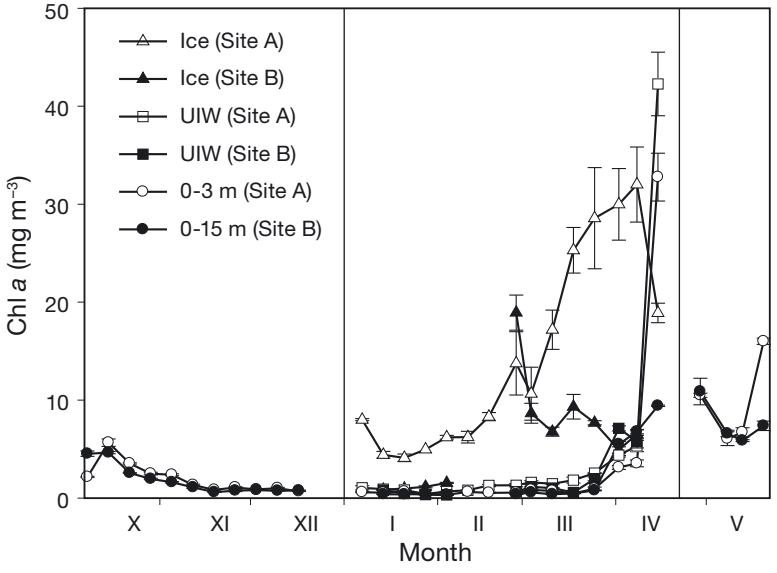

Fig. 2. Mean (±SD) chl *a* concentration throughout the cold-water season from the beginning of October until the end of May in ice, under-ice water (UIW) and the 0–3 m layer at Krogarviken (Site A; open symbols) and in ice, UIW and the 0–15 m layer at Storfjärden (Site B; filled symbols). The period from the beginning of January to the end of April represents the ice-covered season

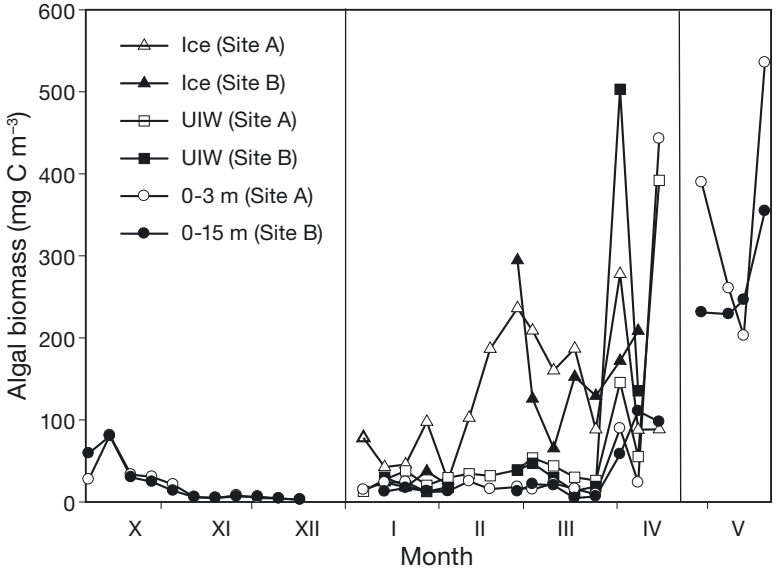

Fig. 3. Total algal biomass throughout the cold-water season from the beginning of October until the end of May in ice, under-ice water (UIW) and the 0–3 m layer at Site A (open symbols) and in ice, UIW and the 0–15 m layer at Site B (filled symbols). The period from the beginning of January to the end of April represents the ice-covered season

was observed 28 Feb 2013 after the reformation of ice, after which the total biomass in ice first decreased and then increased again towards the final ice breakup. An under-ice phytoplankton bloom was observed at both sites in April, and the total biomass in the UIW was 400 and 500 mg C m^{-3} at Sites A and B, respectively. During the phytoplankton spring bloom, the total biomass varied between 200 and 500 mg C m^{-3} and 250 and 350 mg C m^{-3} at Sites A (0–3 m layer) and B (0–15 m), respectively (Fig. 3). Total biomass correlated positively with the chl *a* concentration (Spearman's rank-order correlation; r = 0.822, n = 109, p = 0.01).

Light microscopy

A total of 76 taxa were identified from the samples with inverted light microscopy (Table S2 in Supplement 2). At the beginning of our study, the algal biomass in the water column was dominated by dinoflagellates (37 to 68%), cryptophytes (8 to 11%) and other small flagellates (16 to 29%) identified as classes Prymnesiophyceae (*Chrysochromulina birgeri*) and Prasinophyceae (*Pyramimonas* sp.) in addition to small unidentified flagellates (Fig. 4e,f). *Heterocapsa triquetra*, *Dinophysis* sp. and the '*Scrippsiella*' complex were abundant dinoflagellates, but most dinoflagellates were unidentifiable. Diatoms, both centric (e.g. *Chaetoceros* sp., *Skeletonema* spp.) and pennate (e.g. *Pauliella taeniata* and *Navicula* sp.) and filamentous cyanobacteria (*Planktothrix* sp. and *Aphanizomenon* sp.) were present at both sites. Despite the decreasing biomass during October to December, the algal assemblage in the water column at the beginning of the ice-covered season (7 and 14 Jan 2013) resembled the fall assemblage and was dominated by dinoflagellates (30 to 48%), cryptophytes (~20%) and small unidentified flagellates (28 to 35%) (Fig. 4e,f). The UIW assemblage was also dominated by dinoflagellates (38 to 73%), cryptophytes (11 to 14%) and small unidentified flagellates (14 to 43%) (Fig. 4c,d).

The ice was characterized by low biomass at the beginning of the ice-covered season (7 Jan 2013 to 14 Feb 2013), and the ice algal assemblage resembled the water column assemblage, but the 2 sites differed. In January, the assemblage at Site A was dominated by dinoflagellates (10 to 32%), especially unidentified dinoflagellates and the '*Scrippsiella*' complex. Other abundant microalgae were cryptophytes (12 to 22%), small flagellates (19 to 41%) and cyanobacteria (10 to 29%) (Fig. 4a). Green algae in-

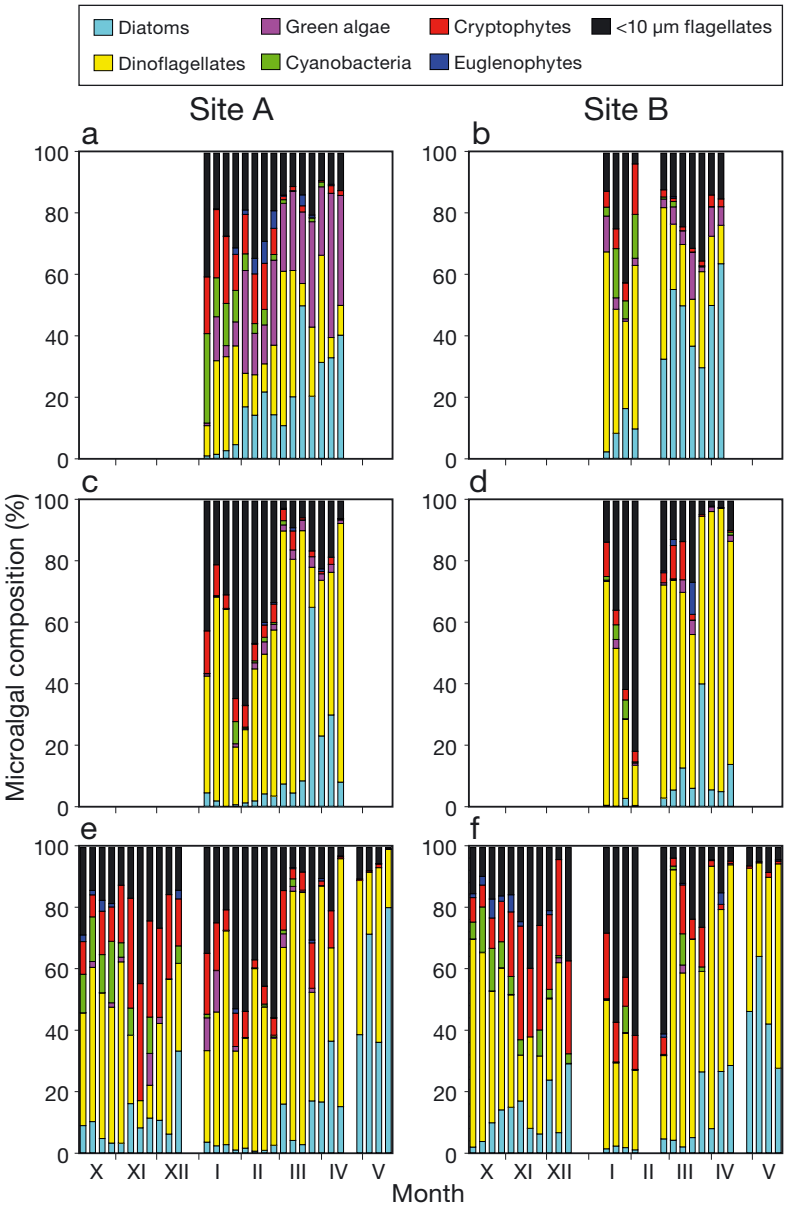

Fig. 4. Seasonal succession of the microalgal assemblage composition (% of total biomass) in (a,b) ice, (c,d) under-ice water (UIW), (e) the 0–3 m layer and (f) 0–15 m layer at Krogarviken (Site A) and Storfjärden (Site B) during October to May

creased in February, especially *Chlamydomonas caudata* and *Klebsormidium flaccidum* and the euglenophytes. At Site B, the assemblage in January was dominated by dinoflagellates (28 to 65%), especially unidentified dinoflagellates and small flagellates (13 to 43%). Cryptophytes, cyanobacteria, green algae and euglenophytes were present, but their biomasses were lower compared to Site A (Fig. 4b). At the end of February, the ice shifted from winter to spring ice, which was characterized by an increase in algal biomass and change in assemblage composition towards the dominance of diatoms and dinoflagellates (Fig. 4a,b). At Site A, green algae, dominated by *K. flaccidum*, was the third largest group (22 to 47%) along with diatoms (11 to 50%) and dinoflagellates (7 to 50%). At Site B, small flagellates remained the third largest group (13 to 36%) along with diatoms (30 to 63%) and dinoflagellates (13 to 49%) (Fig. 4a). The biomass of *Heterocapsa arctica* sub. *frigida* increased, but the dinoflagellate assemblage was dominated by unidentified dinoflagellates and the '*Scrippsiella*' complex. The ice diatom assemblages at both sites were dominated by pennate species including cell chains forming *P. taeniata*/*Navicula* sp. and arborescent colony-forming *Nitzschia frigida*. The centric diatoms were present in the ice throughout the study, but the biomass of centric diatoms, especially from the genera *Chaetoceros* and *Melosira*, increased before ice breakup.

The biomass of dinoflagellates increased in mid-March, and dinoflagellates dominated the algal assemblage in the water column (57 to 81%) (Fig. 4e,f) and UIW (57 to 76%) (Fig. 4c,d). The most dominant dinoflagellates were unidentified dinoflagellates, species from the '*Scrippsiella*' complex and *Peridiniella catenata*. Diatom biomass increased in April, when diatoms formed 8 to 36 and 5 to 30% of the algal biomass in the water column and UIW, respectively. The most abundant diatoms were *Skeletonema* spp., *Chaetoceros* sp. and *P. taeniata*/*Navicula* sp.

The spring bloom assemblage was dominated by dinoflagellates (20 to 66%) and diatoms (28 to 80%) after ice melt (29 Apr 2013 to 22 May 2013) at both sites (Fig. 4e,f). Species from the '*Scrippsiella*' complex, *P. catenata* and *Protoperidinium* sp. dominated the dinoflagellates during the spring bloom. The diatom species *P. taeniata*/*Navicula* sp., abundant in the water column and UIW before ice breakup, was present in the spring bloom at low abundances. *Skeletonema* spp. dominated the diatom assemblage at the beginning of the spring bloom. Later, the diatom assemblage was dominated by the pennate diatom *Diatoma tenuis*.

Taxonomic affiliation of sequences

The taxa identified with light microscopy contributed only a small portion of the OTUs detected in the samples: the sequence data from 58 samples yielded 1039 OTUs at a 97% similarity level. The OTU number varied between samples, from 69 to 259 (mean ± SD = 172 ± 50) sample^{-1}. The taxonomic distribution of assigned OTUs showed that the main groups present at both sampling sites were ciliates, fungi, dinoflagellates, cercozoa, green algae and stramenopiles, a divergent group that includes e.g. diatoms, chrysophytes, bolidophytes, eustigmatophytes, dichtyochophytes and pelagophytes (Fig. S4 in Supplement 2). Here, we concentrate on the predominant dinoflagellates, green algae, diatoms, cryptophytes and haptophytes (Fig. 5a–f). Although mainly phototrophic, these groups may also include mixotrophic, phagotrophic or parasitic species, e.g. certain dinoflagellate species from genus *Gyrodinium* and cryptophytes from genus *Goniomonas*.

Dinoflagellates were the OTU-richest phototrophic group in October to December (with a mean of 34 OTUs in the samples), followed by green algae (20), chrysophytes (15), diatoms (19), cryptophytes (14) and haptophytes (5) (Fig. S4e,f). The most abundant dinoflagellate OTUs were affiliated with *H. triquetra*, *Prorocentrum* sp. and unassigned dinoflagellates. For green algae, *Nannochloris* sp. and *Choricystis* sp. OTUs predominated. The most abundant diatom OTUs were affiliated with centric diatoms and belonged to the genera *Thalassiosira*, *Chaetoceros* and *Skeletonema*. The most abundant cryptophyte OTUs were affiliated with *Falcomonas daucoides*, *Teleaulax acuta* and unassigned cryptophytes, while the most abundant haptophyte OTU was affiliated with *Chrysochromulina birgerii*. Despite the diminishing biomass and changes in assemblage composition, the OTU-based diversity was stable between October and December (repeated-measures ANOVA, $p > 0.05$), and the diversity was higher compared to the water column during January to May (Fig. 6a).

An average of 18 dinoflagellate OTUs were collected from the water column samples (Fig. S4c–f) during the ice-covered season (7 Jan 2013 to 15 Apr 2013), and the most abundant OTUs were affiliated with *Gyrodinium* sp., *Prorocentrum* sp., *H. triquetra* and unassigned dinoflagellates. The mean number of dinoflagellate OTUs in the sea-ice samples was 7 (Fig. S4a,b), and the most abundant OTUs were *Gymnodinium* sp. (*G. dorsalisulcum*), *Apocalathium malmogiense* in addition to *H. triquetra* and unassigned dinoflagellates. The mean number of diatom

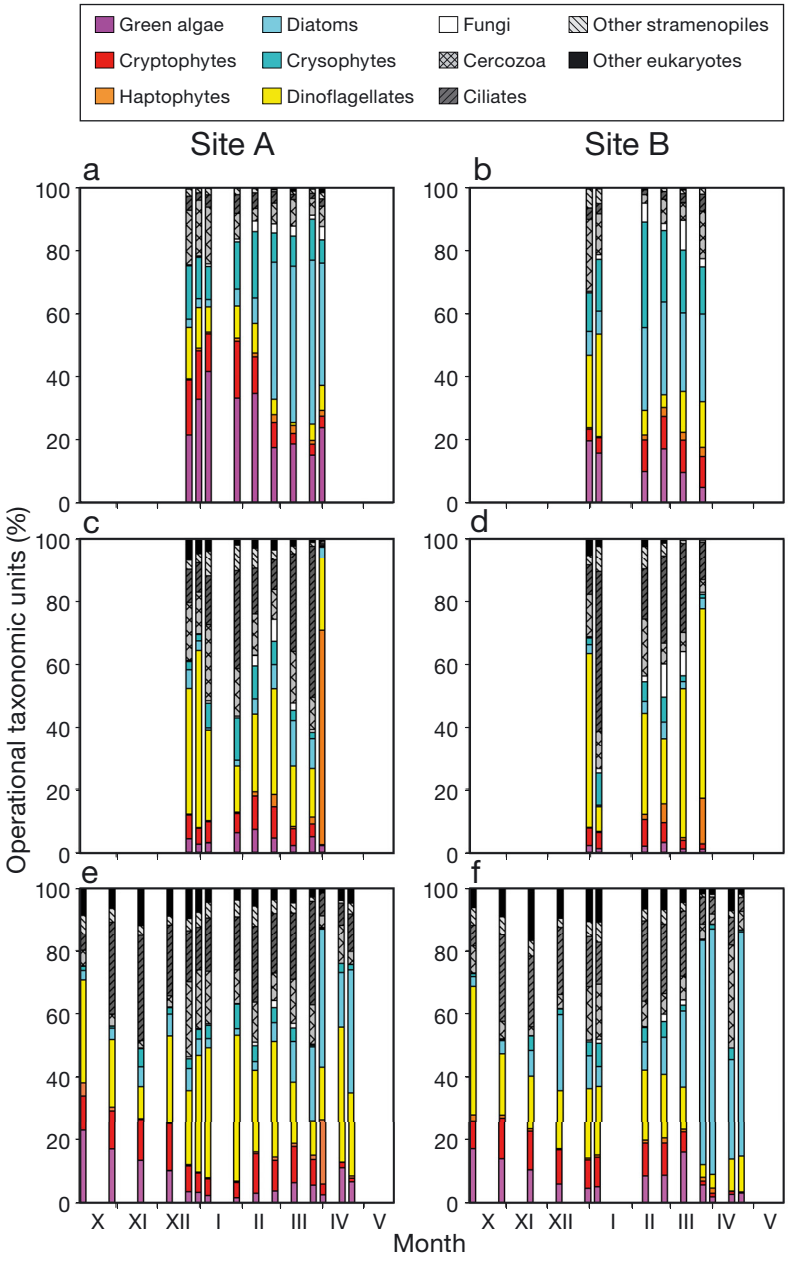

Fig. 5. Seasonal succession of the operational taxonomic unit (OTU) composition (% of the total OTUs) in (a,b) ice, (c,d) under-ice water (UIW), (e) the 0–3 m layer and (f) 0–15 m layer at Krogarviken (Site A) and Storfjärden (Site B) during October to May

OTUs in the water column was 15 (Fig. S4c–f), and the most abundant species were centric diatoms *Thalassiosira guillardii*, *T. hispida*, *Skeletonema* sp. (*S. marinoi*), unassigned Coscinodiscophyceae and pennate *Cymbella* sp. The mean number of diatom OTUs in sea ice was 13 (Fig. S4a,b), and the centric diatom *Chaetoceros socialis* and unassigned Coscinodiscophyceae were the most abundant OTUs. The mean number of green algae OTUs was 17 and 14 in the water column and ice, respectively (Fig. S4a–f), and *Chlamydomonas* sp. was abundant especially in the UIW and sea ice. The mean number of cryptophyte OTUs was 11 in both the water column and the UIW (Fig. S4c–f), and the most abundant OTUs were affiliated with *T. acuta* and unassigned cryptophytes. The sea ice had an average 3 cryptophyte OTUs (Fig. S4a.b), and *Chroomonas* sp. and *F. daucoides* were the most abundant OTUs. Both the UIW and water column averaged 5 haptophyte OTUs (Fig. S4c–f), while sea ice only averaged 3 OTUs (Fig. S4a,b), and similar to the October to December period, the most abundant OTU was *C. birgerii*. The diversity of the water column assemblage during the ice-covered season (7 Jan 2013 to 15 Apr 2013) was lower compared to the water column during October to December, and the diversity in UIW was lower than that in the water column during the ice-covered season (Fig. 6a). OTU-based richness in sea ice was lower compared to the water column and UIW. Evenness, however, was the highest in sea ice (Fig. 6b). Evenness increased during the ice-covered season, especially at Site B.

The mean number of dinoflagellate OTUs was 10 during the spring bloom (29 Apr 2013 to 22 May 2013) (Fig. S4e,f), and unassigned dinoflagellates were the most abundant, in addition to *G. dorsalisulcum*, which was abundant at Site A. The mean number of diatom OTUs was 16 (Fig. S4e,f), and the most abundant species were the centric diatoms *Chaetoceros* sp. (*C. socialis*), *T. guillardii*, *T. hispida*, *Skeletonema* sp. (*S. marinoi*) and the pennate diatom *Cymbella* sp. The mean number of cryptophyte OTUs was 7 (Fig. S4e,f), and the assemblage resembled the UIW assemblage, the abundant species being *F. daucoides*, *T. acuta*, *Chroomonas* sp. and unassigned cryptomonadales. The mean number of haptophyte OTUs was 4 (Fig. S4e,f), and the abundance of *Chrysochromulina* sp. decreased. OTU-based richness increased in spring but, typical for a bloom situation, the evenness of the spring water assemblage was low (Fig. 6a,b).

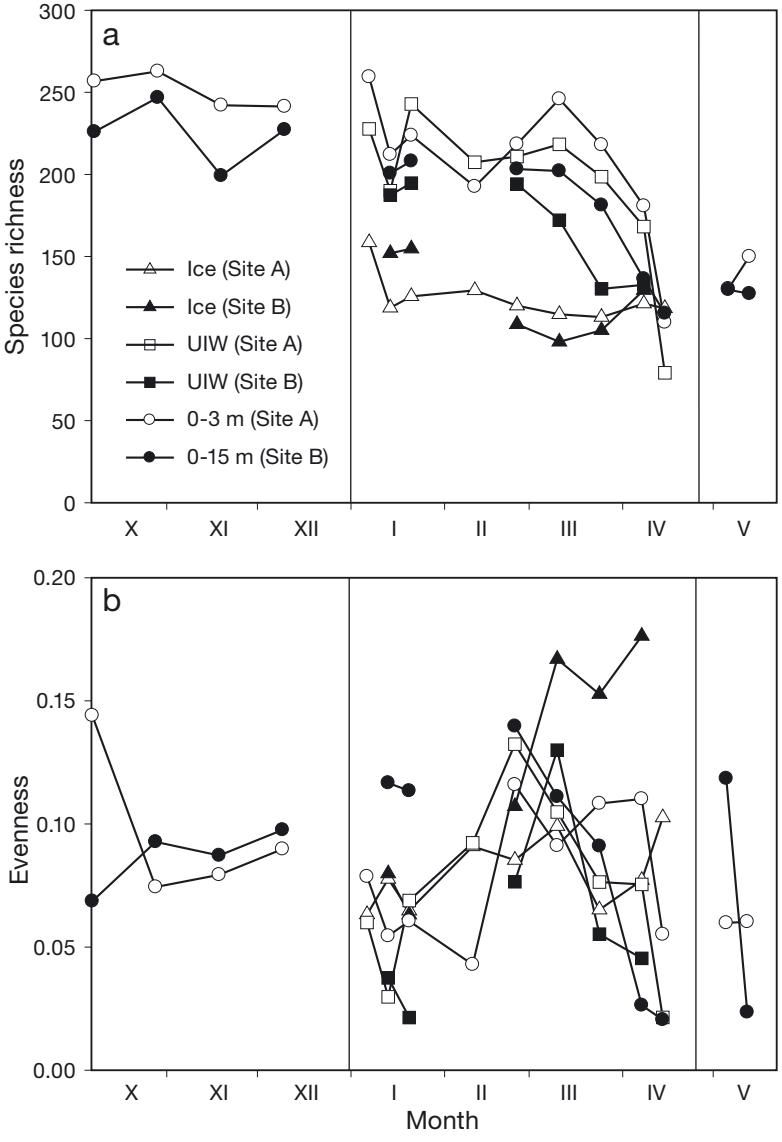

Fig. 6. Comparison of (a) richness and (b) evenness throughout the cold-water season from the beginning of October until the end of May in ice, under-ice water (UIW) and the 0–3 m layer at Site A (open symbols) and in ice, UIW and the 0–15 m layer at Site B (filled symbols). The timeline from the beginning of January to the end of April represents the ice-covered season

Groups

The dendrogram produced from the Bray-Curtis similarity coefficients for the OTUs (size fraction 0.22 o 20 µm) showed 8 clusters at ~55% similarity (Fig. 7a). The clusters followed the *a priori* groups: the fall (8 Oct 2012 to 17 Dec 2012), the water column during the ice-covered season (7 Jan 2013 to 15 Apr 2013), the UIW (7 Jan 2013 to 15 Apr 2013), the ice (7 Jan 2013 to 15 Apr 2013) and the spring bloom (29 Apr 2013 to 22 May 2013), and the groups harboured significantly different assemblage compositions (1-way PERMANOVA, $F = 22.76_{4,54}$, sum of squares = 12.04, within group sum of squares = 5.062, $p < 0.001$). Three extra clusters included 5 transitional samples: 2 early UIW samples, 2 early sea-ice samples and 1 water sample from the winter–spring transition (C14, F14, D13, D14 and F26 in Fig. 7a). In addition, the 3 first UIW samples (F12, C13, F13 in Fig. 7a) clustered with the winter water samples and the 3 final winter water samples (A25, E25, E26 in Fig. 7a; sampled under ice) clustered with an early spring water sample.

The dendrogram based on the microalgal biomasses (including microalgae >20 µm) showed similar clustering as that based on the OTUs (Fig. 7b), and the *a priori* groups based on biomasses harboured significantly different assemblage compositions, except fall and winter water (1-way PERMANOVA, F = 10.23, sum of squares = 12.26, within group sum of squares = 7.572, $p < 0.001$, Bonferroni corrected). Though the differences between the groups were not as clear based on the algal biomass results as they were for the OTU results, the similarity matrixes (used for producing the dendrograms) were related (ρ = 0.5, $p < 0.01$).

DISCUSSION

Our results provide new insight into cold-water season algal succession in the northern Baltic Sea. The temperature and light environments of the Baltic Sea differ from those in polar areas. In our study we distinguished 5 different groups in the microalgae assemblages, 4 in the water column and 1 in the sea ice, from the beginning of October throughout the ice-covered season until the end of May, with significant differences in assemblage composition and diversity. Four of the 5 groups, i.e. the fall (8 Oct 2012 to 17 Dec 2012), the winter and the under-ice water (both 7 Jan 2013 to 15 Apr 2013) and the spring (29 Apr 2013 to 22 May 2013), were observed in the water column. The phytoplankton succession in the water column during the cold-water season in

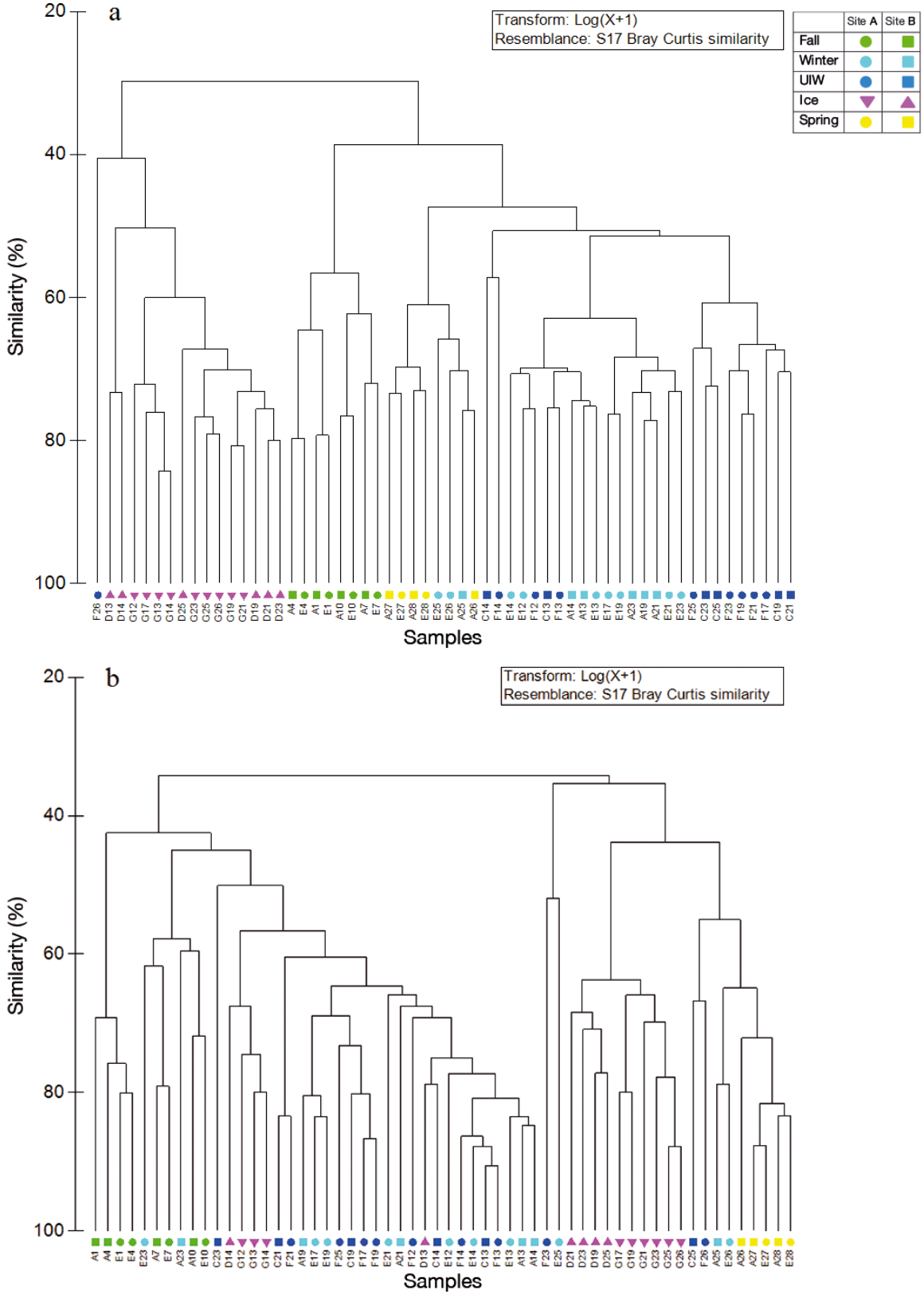

Fig. 7. Dendrograms for percent similarity produced from the Bray-Curtis similarities for (a) operational taxonomic units (OTUs) and (b) microscopy results. UIW: under-ice water

our study coincided with changes in light environment and temperature. The algal assemblage composition of the Baltic Sea changes along a salinity gradient (Gasiūnaitė et al. 2005, Ulanova et al. 2009, Sildever et al. 2015), indicating that salinity is also a potential factor shaping the seasonal algal assemblage succession during the cold-water season between ice and the water column. For example, the seasonal cyanobacteria succession in the water column correlates with both salinity and temperature (Bertos-Fortis et al. 2016), showing that many of the processes affecting microbial assemblages are complex.

At the beginning of October, the assemblage in the water column was dominated by dinoflagellates and other small flagellates belonging to green algae, cryptophytes and haptophytes. Autumnal succession studies from the Baltic Sea are sparse, but an early autumnal bloom dominated by diatoms (dominated by *Chaetoceros* sp. and small cells of *Thalassiosira* spp.) (Bianchi et al. 2002) or small colonial cyanobacteria (Wasmund et al. 2001) was not observed in our study. The amount of light and temperature decreased during the fall and changed the physical environment, resulting in decreased phytoplankton biomass. After the ice formation, small flagellates dominated the algal assemblage in the under-ice water column in concordance with previous wintertime studies (Smith et al. 1991, Clarke & Leakey 1996, Fiala et al. 1998, Ratkova et al. 1999). Flagellate dominance continued until the end of February, probably due to the flagellates' ability to supplement or substitute photosynthesis via mixotrophy and/or heterotrophy as proposed by Mikkelsen et al. (2008).

Różańska et al. (2008) found that nearly every species was observed in both the newly formed sea ice and the water column, while only a few species were found exclusively in the water column. In contrast, Tuschling et al. (2000) and Majaneva et al. (2012b) have shown sea-ice assemblages to differ from those observed in the water column and in the newly formed sea ice. The sea-ice algal assemblage in our study resembled the water column assemblage at the beginning of the ice-covered season and, similar to the water column, was dominated by small flagellates. The lower richness observed in the ice in January compared to the water column based on the OTUs indicates that ice assemblage formation was not unequivocally a non-selective concentrating mechanism during ice formation, as earlier proposed by Garrison et al. (1983), but that each species in the water column was unable to colonize the forming sea ice. However, the selection of diatoms during ice formation into ice, earlier shown by Gradinger & Ikävalko (1998), was not observed in our study, possibly due to the low diatom abundance in the water column. *In situ* ice formation studies are challenging in practice, and consequently, the first ice samples are typically collected days or weeks after ice formation. This is also true for our study. The characteristics of the algal assemblage during ice formation in this study cannot be determined due to possible changes in the assemblage between ice formation and the first sampling.

The succession of the ice algae observed in our study was similar to the succession described in previous studies, beginning with a winter stage with low production, followed by a growth phase and later the melting period, which ends in ice breakup (Haecky & Andersson 1999, Kaartokallio 2004, Granskog et al. 2006, Leu et al. 2015). The low ice algal biomass at the beginning of the ice-covered season has previously been observed in short-term studies performed in the northern Baltic Sea (e.g. Niemi & Åström 1987, Kangas et al. 1993, Piiparinen et al. 2010, Rintala et al. 2010). The algal biomass began increasing towards the spring equinox, and the assemblage changed from a flagellate-dominated assemblage to a dinoflagellate- and diatom-dominated assemblage, showing that early-winter successional species are eliminated by late-winter successional species. The abundant species in the spring ice originated from the initial ice assemblage. The new algal populations could also have been introduced from the UIW (1) due to the upward flux of UIW into the brine channels (Stoecker et al. 1993, 1998), (2) via the UIW microalgae attaching and accumulating to the bottom-ice surface and ultimately freezing into the ice (Syvertsen 1991) or (3) via a combination of both processes.

Spatial differences between the ice algal assemblage compositions were already encountered between the study sites from the beginning of our study. The biomass of the green alga *Klebsormidium flaccidum*, which lives on rocks and other substrates, was higher at Site A than at Site B, indicating that the incorporation of bottom-dwelling species into the ice is more likely in shallow areas. Dinoflagellate cysts are abundant in Arctic and Antarctic sea ice (e.g. Stoecker et al. 1998, Różańska et al. 2008). Dinoflagellate cysts are numerous in the surface sediment of the Baltic Sea (0 to 5 cm) (Sildever et al. 2017), but less is known about the dinoflagellate cysts in Baltic Sea ice. Although dinoflagellates dominated the sea-ice assemblage in our study, the biomass of dinoflagellate cysts accounted for only a small proportion of the total biomass. Previous studies have shown low

cyst-forming dinoflagellate diversity between the salinities of 6 to 10 compared to high diversity when the salinity level approaches 30 (Ellegaard 2000, Sildever et al. 2015), indicating that cyst formation is only a minor survival strategy for dinoflagellates in northern Baltic Sea ice, where the salinity is lower than the oceanic sea ice.

The decrease in ice algal biomass during the end of March and in the beginning of April was followed by a subsequent increase of microalgal biomass in UIW. In concordance with a previous study from the Arctic (Arrigo et al. 2014), the dominant species differed in the water column and ice, indicating that the under-ice bloom was comprised of species able to reproduce in the UIW environment and not of the dominant sea-ice algae. After ice breakup, the subsequent phytoplankton bloom and nitrogen depletion were observed in the water column in concordance with previous studies (e.g. Michel et al. 1993, Kuosa et al. 1997, Haecky et al. 1998, Różańska et al. 2009, Sukhanova et al. 2009, Hodal et al. 2012, Lips et al. 2014), but the intensity of the bloom differed between the sites. The assemblage was dominated by diatoms and dinoflagellates during both spring ice and spring bloom, indicating a seeding effect from the sea ice. However, multivariate analyses showed that species composition was different in the ice compared to the spring bloom, indicating that the spring bloom species were pioneer species of the open-water season. Consequently, as previously suggested by Mikkelsen et al. (2008) and Riaux-Gobin et al. (2011), the spring bloom assemblage was not exclusively formed from sea-ice algae, or at least not from the same dominant species. However, Kremp et al. (2008) showed that the size of inoculum dinoflagellate population and the co-occurring diatoms affects the bloom formation and dominance of the dinoflagellate population. The ice algae that are released from the melting sea ice, which do not contribute to production in the water column, are grazed by pelagic or benthic herbivores. Alternatively, the cells could be exposed to microbial degradation or sedimentation, depending on how well the microalgae maintain their buoyancy in the water column. Padisák et al. (2003) showed that the sinking rate is enhanced in colonial-forming microalgae that lack the symmetric shape of the colony. This could explain the decrease of the arborescent colonies of *Nitzschia frigida* after ice breakup. Elimination by immediate cell lysis due to osmotic shock (Garrison & Buck 1986) is unlikely, especially in the Baltic Sea, as Rintala et al. (2014) showed that direct melting of the Baltic Sea does not cause instant destruction of algal cells. Mild winters are occurring more frequently in the Baltic Sea, and the length of the ice season has decreased by 30 d during the last 100 yr (Merkouriadi & Leppäranta 2014). Winters with no ice cover, and conditions of decreased salinity and increased sea surface temperatures could lead to earlier phytoplankton blooms with increased biomass and smaller phytoplankton taxa, changes that are similar to those described in mesocosm experiments (e.g. Sommer et al. 2007, Winder et al. 2012). A decrease in fresh water ice cover additionally results in a shift from a phytoplankton assemblage dominated by filamentous diatoms to smaller cells (Beall et al. 2016). Ice algal production is estimated to constitute 0.4% of the annual primary production in the Baltic Sea (Haecky & Andersson 1999). Our results show that ice microalgal biomass based on cell enumeration is high compared to phytoplankton biomass, especially at the end of the ice-covered season. However, if ice thickness is less than 0.5 m, as in our study, the contribution of ice algae to total primary production remains low (data not shown). In polar areas where ice cover is thicker, the ice algae may contribute more than 50% to total primary production (Gosselin et al. 1997).

In conclusion, the cold-water season is a dynamic season with various algal assemblages occurring in the sea ice and water column, albeit at low algal biomass. The sea-ice assemblage resembled the water column assemblage, but species richness was lower in the sea ice compared to the water column, indicating that the formation of the ice assemblage was unlikely a non-selective concentrating mechanism during ice formation. Both the water column assemblage and the sea-ice assemblage changed from flagellate-dominated assemblages to diatom-dominated assemblages. However, the sea-ice assemblage formed a significantly different group compared to the water assemblages. In addition, the difference between ice and spring bloom assemblage compositions indicates that sea-ice algae do not have a large seeding effect from the ice. Although the sea-ice assemblage does not greatly contribute to water column phytoplankton growth and spring bloom subsequent to the ice melt, it may contribute greatly to total microalgal biomass during the ice-covered season.

Acknowledgements. The Walter and Andrée de Nottbeck Foundation and University of Helsinki 3-year research grants (Blomster) provided financial support for this work. The field and laboratory work was made possible by the facilities at Tvärminne Zoological Station and the Department of Environmental Sciences, University of Helsinki and the Marine Research Centre, Finnish Environment Institute. We thank Göran Lundberg, Veijo Kinnunen and Dr. Joanna

Norkko for their help in the fieldwork and Mona Aweys for her help in the DNA extractions. Veijo Kinnunen, Mikael Kraft and Jani Ruohola are acknowledged for their help in the microscopy work. In addition, we thank anonymous reviewers for their valuable comments on the manuscript.

LITERATURE CITED

Anderson MJ (2001) A new method for non-parametric multivariate analysis of variance. Austral Ecol 26:32–46

Andersson A, Hajdu S, Haecky P, Kuparinen J, Wikner J (1996) Succession and growth limitation of phytoplankton in the Gulf of Bothnia (Baltic Sea). Mar Biol 126: 791–801

Arrigo KR, Perovich DK, Pickart RS, Brown ZW and others (2014) Phytoplankton blooms beneath the sea ice in the Chukchi Sea. Deep Sea Res II 105:1–16

Beall BFN, Twiss MR, Smith DE, Oyserman BO and others (2016) Ice cover extent drives phytoplankton and bacterial community structure in a large north-temperate lake: implications for a warming climate. Environ Microbiol 18:1704–1719

Bertos-Fortis M, Farnelid HM, Lindh MV, Casini M and others (2016) Unscrambling cyanobacteria community dynamics related to environmental factors. Front Microbiol 7:625

Bianchi TS, Rolff C, Widbom B, Elmgren R (2002) Phytoplankton pigments in Baltic Sea seston and sediments: seasonal variability, fluxes, and transformations. Estuar Coast Mar Sci 55:369–383

Chevenet F, Brun C, Bañuls AL, Jacq B, Christen R (2006) TreeDyn: towards dynamic graphics and annotations for analyses of trees. BMC Bioinformatics 7:439

Chevenet F, Croce O, Hebrard M, Christen R, Berry V (2010) ScripTree: scripting phylogenetic graphics. Bioinformatics 26:1125–1126

Clarke A, Leakey RJG (1996) The seasonal cycle of phytoplankton, macronutrients, and the microbial community in a nearshore Antarctic marine ecosystem. Limnol Oceanogr 41:1281–1294

Comeau AM, Li WKW, Tremblay JE, Carmack EC, Lovejoy C (2011) Arctic Ocean microbial community structure before and after the 2007 record sea ice minimum. PLOS ONE 6:e27492

Dale T, Rey F, Heimdal BR (1999) Seasonal development of phytoplankton at a high latitude oceanic site. Sarsia 84: 419–435

Edgar RC (2013) UPARSE: highly accurate OTU sequences from microbial amplicon reads. Nat Methods 10:996–998

Ellegaard M (2000) Variations in dinoflagellate cyst morphology under conditions of changing salinity during the last 2000 years in the Limfjord, Denmark. Rev Palaeobot Palynol 109:65–81

Fiala M, Kopczynska EE, Jeandel C, Oriol L, Vetion G (1998) Seasonal and interannual variability of size-fractionated phytoplankton biomass and community structure at station Kerfix, off the Kerguelen Islands, Antarctica. J Plankton Res 20:1341–1356

Finni T, Kononen K, Olsonen R, Wallström K (2001) The history of cyanobacterial blooms in the Baltic Sea. Ambio 30:172–178

Garrison DL, Buck KR (1986) Organism losses during ice melting: a serious bias in sea ice community studies. Polar Biol 6:237–239

Garrison DL, Ackley SF, Buck KR (1983) A physical mechanism for establishing algal populations in frazil ice. Nature 306:363–365

Gasiūnaitė ZR, Cardoso AC, Heiskanen AS, Henriksen P and others (2005) Seasonality of coastal phytoplankton in the Baltic Sea: influence of salinity and eutrophication. Estuar Coast Shelf Sci 65:239–252

Gleitz M, Bartsch A, Dieckmann GS, Eicken H (1998) Composition and succession of sea ice diatom assemblages in the eastern and southern Weddell Sea, Antarctica. Antarct Res Ser 73:107–120

Golden KM, Ackley SF, Lytle VI (1998) The percolation phase transition in sea ice. Science 282:2238–2241

Gosselin M, Levasseur M, Wheeler PA, Horner RA, Booth BC (1997) New measurements of phytoplankton and ice algal production in the Arctic Ocean. Deep Sea Res II 44: 1623–1644

Gradinger R, Ikävalko J (1998) Organism incorporation into newly forming Arctic sea ice in the Greenland Sea. J Plant Res 20:871–886

Granskog M, Kaartokallio H, Kuosa H, Thomas DN, Vainio J (2006) Sea ice in the Baltic Sea — a review. Estuar Coast Shelf Sci 70:145–160

Grossmann S, Gleitz M (1993) Microbial responses to experimental sea-ice formation: implications for the establishment of Antarctic sea-ice communities. J Exp Mar Biol Ecol 173:273–289

Guillou L, Bachar D, Audic S, Bass D and others (2013) The protist ribosomal reference database (PR2): a catalog of unicellular eukaryote small sub-unit rRNA sequences with curated taxonomy. Nucleic Acids Res 41: D597–D604

Haecky P, Andersson A (1999) Primary and bacterial production in sea ice in the northern Baltic Sea. Aquat Microb Ecol 20:107–118

Haecky P, Jonsson S, Andersson A (1998) Influence of sea ice on the composition of the spring phytoplankton bloom in the northern Baltic Sea. Polar Biol 20:1–8

Hammer Ø, Harper DAT, Ryan PD (2001) PAST: paleontological statistics software package for education and data analysis. Palaeontol Electronica 4:art4

HELCOM (Helsinki Commission) (1988) Guidelines for the Baltic Monitoring Programme for the third stage. Part D. Biological determinants. Balt Sea Environ Proc 27D: 16–23

Hodal H, Falk-Petersen S, Hop H, Kristiansen S, Reigstad M (2012) Spring bloom dynamics in Kongsfjorden, Svalbard: nutrients, phytoplankton, protozoans and primary production. Polar Biol 35:191–203

Hugerth LW, Muller EEL, Hu YOO, Lebrun LAM and others (2014) Systematic design of 18S rRNA gene primers for determining eukaryotic diversity in microbial consortia. PLOS ONE 9:e95567

Huson DH, Beier S, Flade I, Górska A and others (2016) MEGAN Community Edition — interactive exploration and analysis of large-scale microbiome sequencing data. PLOS Comput Biol 12:e1004957

Kaartokallio H (2004) Food web components, and physical and chemical properties of Baltic Sea ice. Mar Ecol Prog Ser 273:49–63

Kaartokallio H, Tuomainen J, Kuosa H, Kuparinen J and others (2008) Succession of sea-ice bacterial communities in the Baltic Sea fast ice. Polar Biol 31:783–793

Kahru M, Savchuk OP, Elmgren R (2007) Satellite measurements of cyanobacterial bloom frequency in the Baltic

Sea: interannual and spatial variability. Mar Ecol Prog Ser 343:15–23

Kangas P, Alasaarela E, Lax HG, Jokela S, Storgård-Envall C (1993) Seasonal variation of primary production and nutrient concentrations in the coastal waters of Bothnian Bay and The Quark. Aqua Fenn 23:165–176

Klais R, Tamminen T, Kremp A, Spilling K and others (2013) Spring phytoplankton communities shaped by interannual weather variability and dispersal limitation: mechanisms of climate change effects on key coastal primary producers. Limnol Oceanogr 58:753–762

Koroleff F (1976) Determination of nutrients. In: Grasshoff K (ed) Methods of seawater analysis. Verlag Chemie, Weinheim, p 117–181

Koskinen K, Hultman J, Paulin L, Auvinen P, Kankaanpää H (2011) Spatially differing bacterial communities in water columns of the northern Baltic Sea. FEMS Microbiol Ecol 75:99–110

Kozich JJ, Westcott SL, Baxter NT, Highlander SK, Schloss PD (2013) Development of a dual-index sequencing strategy and curation pipeline for analyzing amplicon sequence data on the MiSeq Illumina sequencing platform. Appl Environ Microbiol 79:5112–5120

Krawczyk DW, Witkowski A, Juul-Pedersen T, Arendt KE and others (2015) Microplankton succession in a SW Greenland tidewater glacial fjord influenced by coastal inflows and run-off from the Greenland Ice Sheet. Polar Biol 38:1515–1533

Kremp A, Tamminen T, Spilling K (2008) Dinoflagellate bloom formation in natural assemblages with diatoms: nutrient competition and growth strategies in Baltic spring phytoplankton. Aquat Microb Ecol 50:181–196

Kuosa H, Autio R, Kuuppo P, Setälä O, Tanskanen S (1997) Nitrogen, silicon and zooplankton controlling the Baltic spring bloom: an experimental study. Estuar Coast Shelf Sci 45:813–821

Legrand C, Fridolfsson E, Bertos-Fortis M, Lindehoff E and others (2015) Interannual variability of phyto-bacterioplankton biomass and production in coastal and offshore waters of the Baltic Sea. Ambio 44(Suppl 3):S427–S438

Leu E, Mundy C, Assmy P, Campbell K and others (2015) Arctic spring awakening — steering principles behind the phenology of vernal ice algal blooms. Prog Oceanogr 139:151–170

Lips I, Rünk N, Kikas V, Meerits A, Lips U (2014) High-resolution dynamics of the spring bloom in the Gulf of Finland of the Baltic Sea. J Mar Syst 129:135–149

Lizotte MP (2003) The microbiology of sea ice. In: Thomas DN, Dieckmann GS (eds) Sea ice: an introduction to its physics, chemistry, biology and geology. Blackwell, Malden, MA, p 184–210

Luhtala H, Tolvanen H (2013) Optimizing the use of Secchi depth as a proxy for euphotic depth in coastal waters: an empirical study from the Baltic Sea. ISPRS Int J Geoinf 2: 1153–1168

Majaneva M, Rintala JM, Hajdu S, Hällfors S and others (2012a) The extensive bloom of alternate-stage *Prymnesium polylepis* (Haptophyta) in the Baltic Sea during autumn–spring 2007–2008. Eur J Phycol 47:310–320

Majaneva M, Rintala JM, Piisilä M, Fewer DP, Blomster J (2012b) Comparison of wintertime eukaryotic community from sea ice and open water in the Baltic Sea, based on sequencing of the 18S rRNA gene. Polar Biol 35:875–889

Makarevich PR, Larionov VV, Moiseev DV (2015) Phytoplankton succession in the Ob-Yenisei Shallow zone of the Kara Sea based on Russian databases. J Sea Res 101: 31–40

Meiners K, Vancoppenolle M, Thanassekos S, Dieckmann GS and others (2012) Chlorophyll *a* in Antarctic sea ice from historical ice core data. Geophys Res Lett 39:L21602

Menden-Deuer S, Lessard EJ (2000) Carbon to volume relationships for dinoflagellates, diatoms, and other protist plankton. Limnol Oceanogr 45:569–579

Merkouriadi I, Leppäranta M (2014) Long-term analysis of hydrography and sea-ice data in Tvärminne, Gulf of Finland, Baltic Sea. Clim Change 124:849–859

Michel C, Legendre L, Therriault JC, Demers S, Vandevelde T (1993) Springtime coupling between ice algal and phytoplankton assemblages in southeastern Hudson Bay, Canadian Arctic. Polar Biol 13:441–449

Mikkelsen DM, Rysgaard S, Glud RN (2008) Microalgal composition and primary production in Arctic sea ice: a seasonal study from Kobbefjord (Kangerluarsunnguaq), West Greenland. Mar Ecol Prog Ser 368:65–74

Moreau S, Ferreyra GA, Mercier B, Lemarchand K and others (2010) Variability of the microbial community in the western Antarctic Peninsula from late fall to spring during a low ice cover year. Polar Biol 33:1599–1614

Nicolaus M, Katlein C, Maslanik J, Hendricks S (2012) Changes in Arctic sea ice result in increasing light transmittance and absorption. Geophys Res Lett 39:L24501

Niemi Å (1973) Ecology of phytoplankton in the Tvärminne area, SW coast of Finland I. Dynamics of hydrography, nutrients, chlorophyll *a* and phytoplankton. Acta Bot Fenn 100:1–69

Niemi Å, Åström AM (1987) Ecology of phytoplankton in the Tvärminne area, SW coast of Finland. IV. Environmental conditions, chlorophyll *a* and phytoplankton in winter and spring 1984 at Tvärminne Storfjärd. Ann Bot Fenn 24:333–352

Niemi A, Michel C, Hille K, Poulin M (2011) Protist assemblages in winter sea ice: setting the stage for the spring ice algal bloom. Polar Biol 34:1803–1817

Olenina I, Hajdu S, Edler L, Andersson A and others (2006) Biovolumes and size-classes of phytoplankton in the Baltic Sea. HELCOM Baltic Sea Environ Proc No. 106

Padisák J, Soróczki-Pintér É, Rezner Z (2003) Sinking properties of some phytoplankton shapes and the relation of form resistance to morphological diversity of plankton — an experimental study. Hydrobiologia 500:243–257

Piiparinen J, Kuosa H, Rintala JM (2010) Winter-time ecology in the Bothnian Bay, Baltic Sea: nutrients and algae in fast ice. Polar Biol 33:1445–1461

Popova EE, Yool A, Coward AC, Aksenov YK and others (2010) Control of primary production in the Arctic by nutrients and light: insights from a high resolution ocean general circulation model. Biogeosciences 7:3569–3591

Poulin M, Daugbjerg N, Gradinger R, Ilyash L and others (2011) The pan-Arctic biodiversity of marine pelagic and sea-ice unicellular eukaryotes: a first-attempt assessment. Mar Biodivers 41:13–28

Ratkova TN, Wassmann P (2005) Sea ice algae in the White and Barents seas: composition and origin. Polar Res 24: 95–110

Ratkova TN, Wassmann P, Verity PG, Andreassen IJ (1999) Abundance and biomass of pico-, nano-, and microplankton on a transect across Nordvestbanken, north Norwegian shelf, in 1994. Sarsia 84:213–225

Riaux-Gobin C, Poulin M, Dieckmann G, Labrune C, Vétion G (2011) Spring phytoplankton onset after the ice break-

up and sea-ice signature (Ade'lie Land, East Antarctica). Polar Res 30:5910
Riedel A, Michel C, Gosselin M, LeBlanc B (2008) Winter–spring dynamics in sea-ice carbon cycling in the coastal Arctic Ocean. J Mar Syst 74:918–932
Rintala JM, Piiparinen J, Uusikivi J (2010) Drift-ice and under-ice water communities in the Gulf of Bothnia (Baltic Sea). Polar Biol 33:179–191
Rintala JM, Piiparinen J, Blomster J, Majaneva M and others (2014) Fast direct melting of brackish sea-ice samples results in biologically more accurate results than slow buffered melting. Polar Biol 37:1811–1822
Różańska M, Poulin M, Gosselin M (2008) Protist entrapment in newly formed sea ice in the coastal Arctic Ocean. J Mar Syst 74:887–901
Różańska M, Gosselin M, Poulin M, Wiktor JM, Michel C (2009) Influence of environmental factors on the development of bottom ice protist communities during the winter–spring transition. Mar Ecol Prog Ser 386:43–59
Sildever S, Andersen TJ, Ribeiro S, Ellegaard M (2015) Influence of surface salinity gradient on dinoflagellate cyst community structure, abundance and morphology in the Baltic Sea, Kattegat and Skagerrak. Estuar Coast Shelf Sci 155:1–7
Sildever S, Kremp A, Enke A, Buschmann F and others (2017) Spring bloom dinoflagellate cyst dynamics in three eastern sub-basins of the Baltic Sea. Cont Shelf Res 137:46–55
Sime-Ngando T, Gosselin M, Juniper SK, Levasseur M (1997) Changes in sea-ice phagotrophic microprotists (20–200 µm) during the spring algal bloom, Canadian Arctic Archipelago. J Mar Syst 11:163–172
Smith WO, Brightman RI, Booth BC (1991) Phytoplankton biomass and photosynthetic response during the winter-spring transition in the Fram Strait. J Geophys Res Oceans 96:4549–4554
Sommer U, Gliwicz ZM, Lampert W, Duncan A (1986) PEG-model of seasonal succession of planktonic events in fresh waters. Arch Hydrobiol 106:433–471
Sommer U, Aberle N, Engel A, Hansen T and others (2007) An indoor mesocosm system to study the effect of climate change on the late winter and spring succession of Baltic Sea phyto- and zooplankton. Oecologia 150:655–667
Stoecker DK, Buck KR, Putt M (1992) Changes in the sea-ice brine community during the spring-summer transition, McMurdo Sound, Antarctica. I. Photosynthetic protists. Mar Ecol Prog Ser 84:265–278
Stoecker DK, Buck KR, Putt M (1993) Changes in the sea-ice brine community during the spring-summer transition McMurdo Sound, Antarctica. II. Phagotrophic protists. Mar Ecol Prog Ser 95:103–113
Stoecker DK, Gustafson DE, Black MMD, Baier CT (1998) Population dynamics of microalgae in the upper land-fast sea ice at a snow-free location. J Phycol 34:60–69
Sukhanova IN, Flint MV, Pautova LA, Stockwell DA and others (2009) Phytoplankton of the western Arctic in the spring and summer of 2002: structure and seasonal changes. Deep Sea Res II 56:1223–1236
Svedén JB, Walve J, Larsson U, Elmgren R (2016) The bloom of nitrogen-fixing cyanobacteria in the northern Baltic Proper stimulates summer production. J Mar Syst 163: 102–112
Syvertsen EE (1991) Ice algae in the Barents Sea: types of assemblages, origin, fate and role in the ice-edge phytoplankton bloom. Polar Res 10:277–287
Thomson PG, McMinn A, Kiessling I, Watson M, Goldsworthy PM (2006) Composition and succession of dinoflagellates and chrysophytes in the upper fast ice of Davis Station, East Antarctica. Polar Biol 29:337–345
Tuschling K, von Juterzenka K, Okolodkov YB, Anoshkin A (2000) Composition and distribution of the pelagic and sympagic algal assemblages in the Laptev Sea during autumnal freeze-up. J Plant Res 22:843–864
Ulanova A, Busse S, Snoeijs P (2009) Coastal diatom-environment relationships in the brackish Baltic Sea. J Phycol 45:54–68
Ütermöhl H (1958) Zur Vervollkommnung der quantitativen Phytoplankton-Methodik. Mitt Int Ver Theor Angew Limnol 9:1–38
Wasmund N, Uhlig S (2003) Phytoplankton trends in the Baltic Sea. ICES J Mar Sci 60:177–186
Wasmund N, Voss M, Lochte K (2001) Evidence of nitrogen fixation by non-heterocystous cyanobacteria in the Baltic Sea and re-calculation of a budget of nitrogen fixation. Mar Ecol Prog Ser 214:1–14
Winder M, Berger SA, Lewandowska A, Aberle N and others (2012) Spring phenological responses of marine and freshwater plankton to changing temperature and light conditions. Mar Biol 159:2491–2501
Zhang Z, Schwartz S, Wagner L, Miller W (2000) A greedy algorithm for aligning DNA sequences. J Comput Biol 7: 203–214

Editorial responsibility: Toshi Nagata, Kashiwa, Japan

Submitted: June 14, 2017; Accepted: May 21, 2018
Proofs received from author(s): June 29, 2018